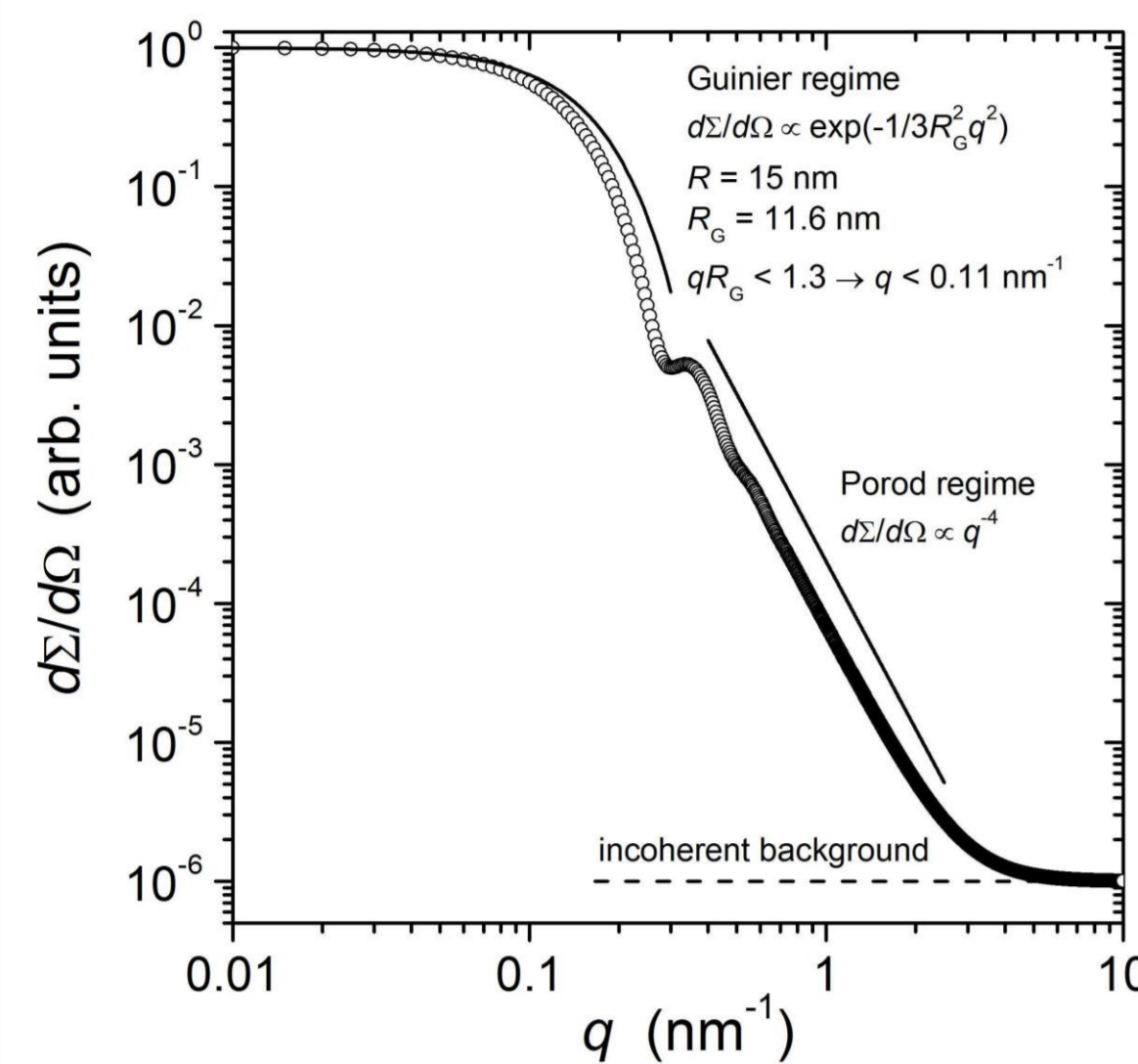


I. Introduction

We introduce the Guinier law for the case of magnetic SANS and provide an analysis of experimental data on a Nd-Fe-B-based nanocomposite and on a rare-earth-free MnBi permanent magnet. The robustness of this novel approach is discussed and the quantities derived are analyzed in the framework of the existing research literature.

II. Nuclear SANS



- The “conventional” Guinier Law: $\frac{d\Sigma}{d\Omega}(q) \simeq \frac{d\Sigma}{d\Omega}(0)e^{-\frac{1}{3}q^2 R_G^2}$, where R_G is the radius of gyration, is applicable to dilute, monodisperse and randomly oriented particle solutions.
- $R_G^2 = \frac{\int_0^D r^2 p(r) dr}{2 \int_0^D p(r) dr}$ is the normalized second moment of the distance distribution function $p(r)$ of the particle around the center of its scattering length density distribution [1]
- $R_G^2 = \frac{3}{5}R_0^2$ for a dilute solution of monodisperse spheres of radius R_0 .

Deviations from the Guinier behavior in the low- q range are usually interpreted as evidence for the presence of attractive/repulsive interparticle interactions.

III. Theory

In the approach-to-saturation regime, the total (nuclear and magnetic) SANS cross section $d\Sigma/d\Omega$ can be expressed as the sum of the residual ($d\Sigma_{res}/d\Omega$) and the spin-misalignment ($d\Sigma_{SM}/d\Omega$) cross sections [2,3]:

$$\frac{d\Sigma}{d\Omega}(q, H_i) = \frac{d\Sigma_{res}}{d\Omega}(q) + \frac{d\Sigma_{SM}}{d\Omega}(q, H_i) = \frac{d\Sigma_{res}}{d\Omega}(q) + S_H(q)R_H(q, H_i)$$

- $R_H(q, H_i)$ is the (dimensionless) micromagnetic response function
- $S_H(q)$ is the anisotropy-field scattering function
- H_i is the internal magnetic field, $H_i = H_0 - NM_s$
- H_0 is the external magnetic field
- N is the demagnetizing factor and
- M_s is the saturation magnetization.

In the following, we consider the low- q behavior of the spin-misalignment SANS cross section $d\Sigma_{SM}/d\Omega = S_H(q)R_H(q, H_i)$.

III.1 Low- q behavior of the response function $R_H(q \rightarrow 0, H_i)$:

$R_H = \frac{p^2(q, H_i)}{2}$, with $p(q, H_i) = \frac{M_s}{H_i(1+l_H^2 q^2)}$, micromagnetic exchange length $l_H = \sqrt{\frac{2A}{\mu_0 M_s H_i}}$ characterizes the field-dependent size of perturbed regions around microstructural defects.

- Taylor expansion of R_H around $q = 0$ yields

$$R_H(q) \simeq \frac{p_0^2}{2} (1 - 2l_H^2 q^2) \simeq \frac{p_0^2}{2} e^{-\frac{1}{3}6l_H^2 q^2}$$

III.2 Low- q behavior of the scattering function $S_H(q \rightarrow 0)$:

- The function $S_H(q)$ equals the magnitude square of the total magnetic anisotropy field Fourier component of the sample:

$$S_H \sim \left| \tilde{\mathbf{H}}_p(\mathbf{q}) \right|^2 = \left| \sum_{i=1}^N \tilde{\mathbf{H}}_{p,i}(\mathbf{q}) \right|^2,$$

where $\tilde{\mathbf{H}}_{p,i}(\mathbf{q})$ represents the anisotropy field Fourier coefficient of the defect i (e.g., an individual grain).

- Assuming random crystalline anisotropy, terms $\tilde{\mathbf{H}}_{p,i} \cdot \tilde{\mathbf{H}}_{p,j}$ with $i \neq j$ vanish (take both signs with equal probability) and, hence, S_H simplifies to:

$$S_H \sim \sum_{i=1}^N \left| \tilde{\mathbf{H}}_{p,i}(\mathbf{q}) \right|^2.$$

- If each grain is a single crystal (constant anisotropy field), then S_H of the sample can be computed from the knowledge of the single grain case. For a homogeneous particle, $\tilde{\mathbf{H}}_p(\mathbf{q})$ simplifies to the following form factor integral [3,4]:

$$\tilde{\mathbf{H}}_p(\mathbf{q}) = \frac{\mathbf{H}_{p,i}}{(2\pi)^{3/2}} \int_{V_{p,i}} e^{-i\mathbf{q}\mathbf{r}} d^3r.$$

This expression is identical (except for the prefactor) to the well known nuclear scattering amplitude of particle scattering; therefore asymptotic results from the nuclear scattering theory at small and large q are directly transferable.

- In particular, $S_H \propto |\tilde{\mathbf{H}}_p|^2$ is related to the “radius of gyration” R_{GH} of the magnetic anisotropy field via:

$$S_H(q) \simeq S_H(0)e^{-\frac{1}{3}q^2 R_{GH}^2}$$

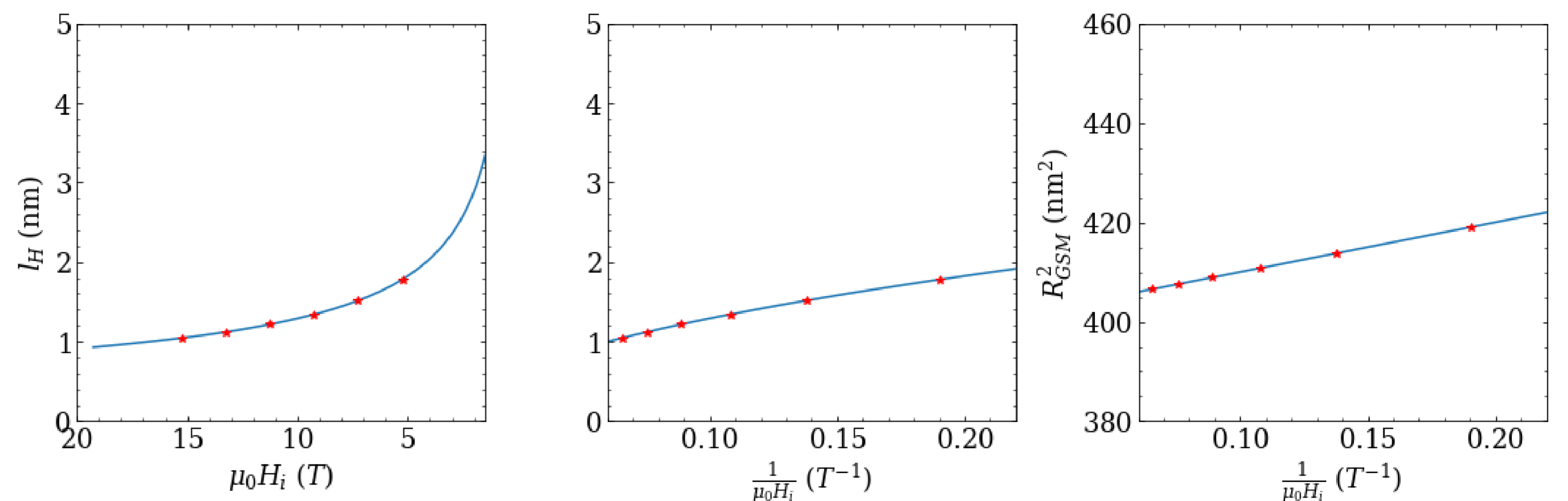
III.3 Resulting low- q behavior of the spin-misalignment cross section

$$\frac{d\Sigma_{SM}(q)}{d\Omega} = S_H(q) * R_H(q, H_i) \simeq S_H(0)e^{-\frac{1}{3}q^2 R_{GH}^2} * \frac{p_0^2}{2} e^{-\frac{1}{3}6l_H^2 q^2} = \frac{d\Sigma_{SM}}{d\Omega}(0)e^{-\frac{1}{3}q^2 R_{GSM}^2}$$

Here, R_{GSM} is a field-dependent “radius of gyration” of spin misalignment defined as:

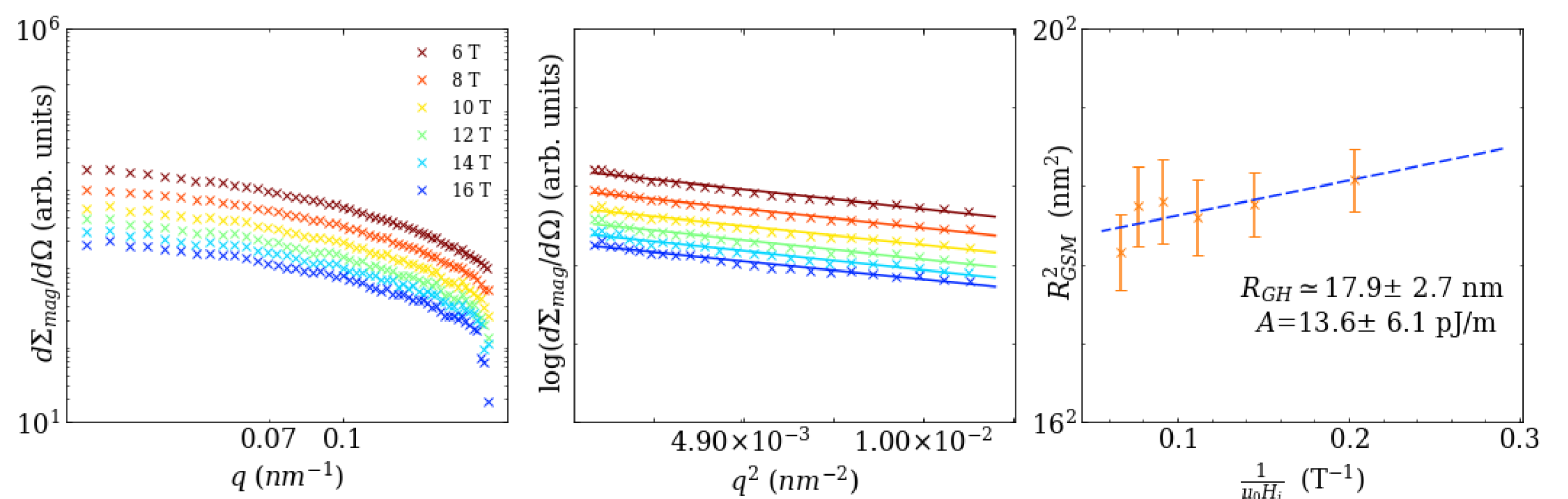
$$R_{GSM}^2(H_i) = R_{GH}^2 + 6l_H^2 = R_{GH}^2 + \frac{12A}{\mu_0 M_s H_i}$$

$R_{GSM}^2(H_i)$ can be obtained from the analysis of field-dependent $\frac{d\Sigma_{SM}}{d\Omega}$ data.

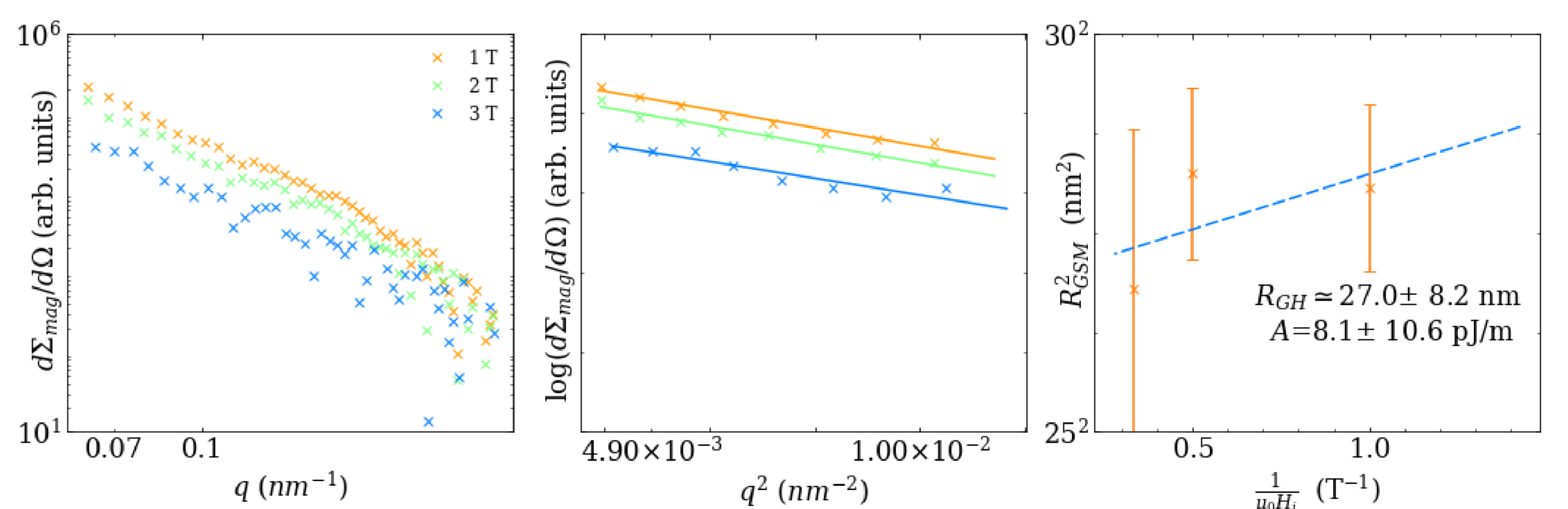


Plots of l_H as a function of the internal field indicate that in the experimentally accessed range of [5] (*) the variation of l_H is very small, respectively, the variation of R_{GSM}^2 would be small as well. ($A = 12.5$ pJ/m; $\mu_0 M_s = 1.5$ T; $N = 0.5$ were used).

IV. Experimental Results



Summary plots of the Nd-Fe-B-based hard magnetic composite. The value obtained for the exchange stiffness constant $A \simeq 13.6 \pm 6.2$ pJ/m coincides with the value obtained via micromagnetic route ($A_{\mu mag} \simeq 13.1 \pm 3.2$ pJ/m) and the radius of gyration is comparable with the particle size $d \simeq 22$ nm [5]. (All the sample and material constants ($\mu_0 M_s$, N) as in [5]).



Summary plots of the MnBi rare-earth-free permanent magnet. The value obtained for the exchange stiffness constant $A \simeq 8.1 \pm 10.6$ pJ/m coincides with the values quoted before [6,7] ($A \simeq 8$ pJ/m). High relative error is due to a small experimentally accessed field variation in this experiment. Additional measurements are ongoing.

V. Summary

We have introduced the magnetic Guinier law on the conceptual level and tested the robustness of the procedure using magnetic SANS data of a Nd-Fe-B-based and rare-earth-free MnBi permanent magnet. In both cases, the obtained values of the exchange stiffness constant are in perfect agreement with existing data in the literature and the radius of gyration of the magnetic anisotropy field was demonstrated to be comparable with the particle size of the nanocrystalline magnet. A broad range of experimentally accessible internal fields is of paramount importance for the subsequent numerical analysis.

References

- [1] D.I. Svergun and M.H.J. Koch, Rep. Prog. Phys. **66**, 10 (2003).
- [2] D. Honecker and A. Michels, Phys. Rev. B **87**, 224426 (2013).
- [3] A. Michels, J. Phys. Condens. Matter. **38**, 26 (2014); S. Mühlbauer et al., Rev. Mod. Phys. **91**, 015004 (2019).
- [4] J. Weissmüller et al., Phys. Rev. B **63**, 214414 (2001).
- [5] J.-P. Bick et al., Appl. Phys. Lett. **102**, 022415 (2013).
- [6] X. Guo et al., Phys. Rev. B **46**, 14578 (1992).
- [7] S. Muralidhar et al., Phys. Rev. B **95**, 024413 (2017).

We acknowledge the financial support from the Fonds National de la Recherche Luxembourg (AFR Individual 12417141).